Journal of Metals, Materials and Minerals, 37(1), e2650, 2027

Supplementary Information

Synchrotron X-ray tomography and functional evaluations of lead-free piezoceramic-filled natural rubber composites

Chotiros DOKKHAN[1], Sirichai PATTANAWANIDCHAI[1], Chutima SAEHENG[1], Phakkhananan PAKAWANIT[2], Chumpon WICHITTANAKOM[3], and Jirapa TANGSRITRAKUL[4,*]

[1] *National Metal and Materials Technology Center, Thailand Science Park, Pathum Thani, 12120, Thailand*
[2] *Synchrotron Research and Applications Division, Synchrotron Light Research Institute, Nakhon Ratchasima, 30000, Thailand*
[3] *Department of Physics, Faculty of Science and Technology, Thammasat University, Pathum Thani, 12120, Thailand*
[4] *Department of Materials and Textile Technology, Faculty of Science and Technology, Thammasat University, Pathum Thani, 12120, Thailand*

***Corresponding author e-mail**: tjirapa@tu.ac.th

Received date:
11 February 2026
Revised date:
17 August 2026
Accepted date:
23 October 2026

Keywords:
Flexible electronics;
Lead-free piezoceramic;
BCZT;
Rubber composites;
Synchrotron X-ray tomography

Abstract

Flexible piezoelectric composite materials have gained increasing attention due to their widespread applications in modern electronic devices such as energy harvesters, dielectric capacitors, or wearable sensors. In this work, flexible piezoelectric composites were developed by incorporating BCZT lead-free piezoceramic fillers into a flexible NR matrix (NR/BCZT composites) with BCZT content ranging from 0 phr to 60 phr (referred as 0BCZT to 60BCZT). Additionally, the structure-property relationships of the NR/BCZT composites were evaluated using synchrotron X-ray tomographic microscopy (SR-XTM), in conjunction with various materials characterization techniques. This work found that the addition of BCZT filler into NR reduced cure time from 14.01 min (0BCZT) to 11.18 min (60BCZT), whereas hardness of the NR/BCZT composites increased from 40.18±0.08 to 45.92±0.11 with increasing BCZT content from 0 phr to 60 phr, respectively. Conversely, the tensile strength of the NR/BCZT composites at all compositions was lower than that of pure NR (tensile strength of 0BCZT = 24.70±2.56 MPa), except for the 30BCZT composite, which exhibited strong adhesion between the BCZT filler and the NR matrix and resulted in the observed highest tensile strength of 26.88±0.90 MPa. Interestingly, no increase in dielectric permittivity occurred at a low BCZT loading of 15 phr, while a significant enhancement from 2.76±0.13 to 3.34±0.08 was observed when the BCZT content was further increased from 15 phr to 30 phr, respectively. The filler dispersion in the NR matrix was investigated using synchrotron X-ray tomographic microscopy (SR-XTM), combined with quantitative analysis of SEM images. The results showed that, the interparticle spacing decreased with increasing the BCZT content in the NR/BCZT composites. This reduction in the interparticle spacing play an important role in the observed electrical properties of the NR/BCZT composites. These findings help to provide a better understanding of the development of lead-free piezoceramic-filled natural rubber composites.

1. Supporting information of the quantitative FTIR analysis

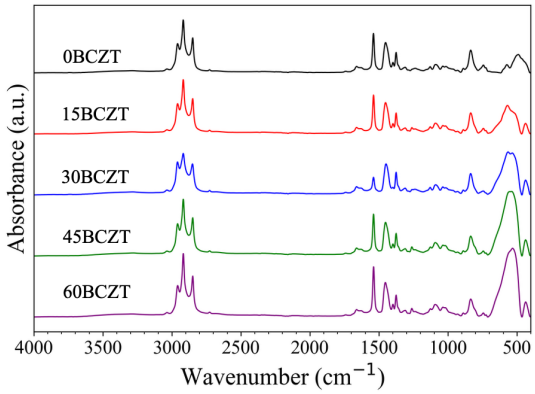


Figure S1. The corresponding FTIR spectra of the NR/BCZT composites converted from transmittance to absorbance mode for quantitative analysis.

Table S1. Summary of the calculated peak areas of the NR matrix (at wavenumber ~837 cm^{-1}), the BCZT filler (at wavenumber between 570 cm^{-1} and 597 cm^{-1}), and the corresponding peak area ratio (R), defined as the peak area of the BCZT filler divided by that of the NR matrix for the NR/BCZT composites with BCZT loading ranging from 0 phr to 60 phr.

Composition	Peak area [Abs·cm^{-1}]		Peak ratio (R)
	NR matrix	BCZT filler	
0BCZT	2.84	0.00	0.00
15BCZT	2.95	12.94	4.38
30BCZT	2.70	22.33	8.27
45BCZT	2.73	33.41	12.26
60BCZT	2.57	35.14	13.66

2. Supporting information of characterization of the NR/BCZT composites

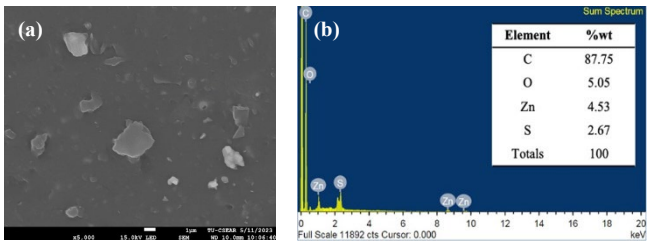


Figure S2. (a) SEM images of the 0BCZT sample, and (b) corresponding Energy dispersive x-ray spectroscopy (EDS) analysis.

3. Supporting information of quantitative SEM image analysis.

3.1 Image-processing procedure

Scanning electron microscopy (SEM) images were quantitatively analyzed to characterize the spatial distribution of BCZT particles dispersed within the natural rubber (NR) matrix. Image analysis was performed using ImageJ/Fiji software (https://imagej.net/ij/). Prior to particle analysis, each SEM micrograph was spatially calibrated using the scale bar embedded in the image so that all measured dimensions were expressed in micrometers (μm) and areas in square micrometers (μm^2).

The SEM images were converted to 8-bit grayscale images, followed by adjustment of the image threshold to distinguish BCZT particles from the surrounding NR matrix. The threshold level was selected to provide the best correspondence between the segmented particle boundaries and the particles visually observed in the original SEM micrograph. When neighboring particles were in direct contact and could be reasonably distinguished as separate objects, a watershed separation procedure was applied with caution to minimize artificial particle splitting.

After image segmentation, individual particles were identified using the "Analyze Particles" function in ImageJ. For each detected particle, the projected particle area (A_i in μm^2), and centroid coordinates (X_i and Y_i in μm) were recorded. The centroid coordinates represent the geometric center of each particle in the two-dimensional SEM image. The measured values were subsequently calculated into the equivalent particle diameter, particle size distribution, nearest-neighbor distance, and descriptive statistical parameters [28–30].

3.2 Image-processing results

Quantitative SEM image analysis was conducted for the 30BCZT and 45BCZT composites to compare the particle size and spatial distribution of BCZT within the NR matrix. The other compositions (0BCZT, 15BCZT, and 60BCZT) were examined qualitatively from the SEM micrographs but were not subjected to quantitative particle analysis. Therefore, the following discussion of equivalent particle diameter, particle size distribution (PSD), and nearest-neighbor distance (NND) focuses specifically on 30BCZT and 45BCZT. A total of 148 particles were identified in the analyzed SEM image of 30BCZT, whereas 286 particles were identified for 45BCZT. The statistical parameters derived from the image analysis are summarized in Table S2.

Table S2. Statistical parameters of BCZT particle size and nearest-neighbor distance in the NR/BCZT composites at BCZT loading of 30 phr and 45 phr.

Parameter	30BCZT	45BCZT
Number of detected particles, N	148	286
Mean particle area (μm^2)	0.83 ± 0.76	0.829 ± 0.72
Median particle area (μm^2)	0.58	0.62
Mean equivalent diameter (μm)	0.93 ± 0.42	0.94 ± 0.41
Median equivalent diameter, D50 (μm)	0.86	0.89
D10 (μm)	0.47	0.47
D90 (μm)	1.57	1.51
Minimum equivalent diameter (μm)	0.34	0.34
Maximum equivalent diameter (μm)	2.44	2.26
Mean NND (μm)	2.36 ± 1.00	1.66 ± 0.69
Median NND (μm)	2.09	1.52
Minimum NND (μm)	0.96	0.59
Maximum NND (μm)	6.44	5.52